Synthesizing sources in magnetics: a benchmark problem

Received 5 May 2021
Revised 28 July 2021
7 September 2021
Accepted 9 September 2021

Synthesizing sources in magnetics: a benchmark problem

Piergiorgio Alotto
Dipartimento di Ingegneria Industriale, Università di Padova, Padua, Italy

Paolo Di Barba
Department of Electrical, Computer and Biomedical Engineering, University of Pavia, Pavia, Italy

Alessandro Formisano
Department of Industrial and Information Engineering, Universita' degli Studi della Campania "Luigi Vanvitelli", Aversa, Italy

Gabriele Maria Lozito
Dipartimento di Ingegneria dell'Informazione, Università degli Studi di Firenze, Firenze, Italy

Raffaele Martone
Department of Industrial and Information Engineering, Università degli Studi della Campania Luigi Vanvitelli, Aversa, Italy

Maria Evelina Mognaschi
Department of Electrical, Computer and Biomedical Engineering, University of Pavia, Pavia, Italy

Maurizio Repetto
Dipartimento Energia, Politecnico di Torino, Turin, Italy

Alessandro Salvini
Dipartimento di Ingegneria, Università degli Studi Roma Tre, Rome, Italy, and

Antonio Savini
Department of Electrical, Computer and Biomedical Engineering, Universita degli Studi di Pavia, Pavia, Italy

Abstract

Purpose – Inverse problems in electromagnetism, namely, the recovery of sources (currents or charges) or system data from measured effects, are usually ill-posed or, in the numerical formulation, ill-conditioned and

COMPEL - The international journal for computation and mathematics in electrical and electronic engineering
Vol. 40 No. 6, 2021
pp. 1084-1103
Emerald Publishing Limited
0332-1649
DOI 10.1108/COMPEL-05-2021-0156

require suitable regularization to provide meaningful results. To test new regularization methods, there is the need of benchmark problems, which numerical properties and solutions should be well known. Hence, this study aims to define a benchmark problem, suitable to test new regularization approaches and solves with different methods.

Design/methodology/approach – To assess reliability and performance of different solving strategies for inverse source problems, a benchmark problem of current synthesis is defined and solved by means of several regularization methods in a comparative way; subsequently, an approach in terms of an artificial neural network (ANN) is considered as a viable alternative to classical regularization schemes. The solution of the underlying forward problem is based on a finite element analysis.

Findings – The paper provides a very detailed analysis of the proposed inverse problem in terms of numerical properties of the lead field matrix. The solutions found by different regularization approaches and an ANN method are provided, showing the performance of the applied methods and the numerical issues of the benchmark problem.

Originality/value – The value of the paper is to provide the numerical characteristics and issues of the proposed benchmark problem in a comprehensive way, by means of a wide variety of regularization methods and an ANN approach.

Keywords Current synthesis, Inverse magnetostatics, Regularization methods, Finite elements, Inverse problems, Finite element analysis, Magnetic device

Paper type Research paper

1. Introduction

Recovering a current distribution from field measurements can be formulated as a source synthesis problem (Isakov, 1990). Inverse problems of this kind are usually ill-conditioned due to the presence of multiple solutions matching the field measurements. With respect to this lack of solution uniqueness, a regularization method needs be used to pick up a single, stable solution.

From literature, many approaches are available, ranging from the standard Tikhonov's regularization to the truncated singular value decomposition (Hansen, 1997) (in the case of linear problems) up to regression-based statistical approaches (Kaipio and Sommersalo, 2005; Formisano, 2019) and the more recent data-based solutions (Khan *et al.*, 2019). In this paper, we propose a simple yet descriptive magnetostatic benchmark problem, which can be used as a testbed to compare different regularization methods.

The case study considered in this paper extends the benchmark proposed by some of the authors in Di Barba *et al.* (2020). While in the former, the geometry of a multi-turn winding generating a uniform field from a given current distribution was searched for, in this work, in contrast, the geometry of the winding is given, while the current distribution is unknown. Therefore, the contribution here proposed is new in terms of both problem formulation (current synthesis instead of shape synthesis) and solution methods (regularization techniques and of optimization algorithms).

The paper is thus organized as follows. in Section 2, the proposed benchmark problem is introduced, in Section 3, the properties of the lead field matrix are shown, then in Sections 4 and 5, a review of some regularization and artificial neural network (ANN) approaches is presented and finally, in Section 6, a comparison of the performance for the introduced approaches on the benchmark problem is discussed, to highlight advantages and drawbacks of each of them.

2. Benchmark problem

2.1 Forward problem

A multi-turn air-cored winding is considered [Figure 1(a)]. The winding, which is composed of $n_t = 20$ independent turns, is suitable for *in vitro* experiments of magneto-fluid hyperthermia.

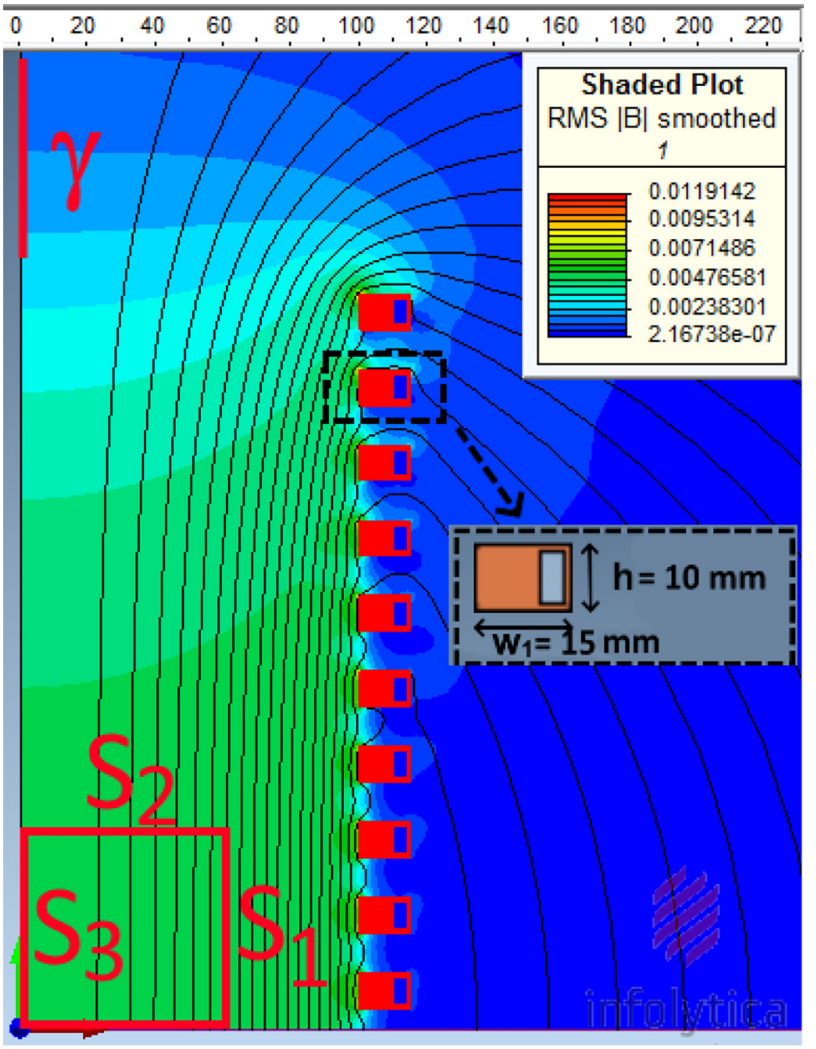

Figure 1.
Geometry, controlled regions and magnetic flux lines

The direct problem, i.e. computing the flux density **B**, given the DC source current density **J** and the coil geometry, is defined as an axisymmetric system, in static conditions. No polarizable magnetic materials are present, and the problem can be considered linear. Notwithstanding the absence of ferromagnetic materials, due to the hollow shape of the conductors, the forward field analysis is better approached by the finite element (FE) method. In this model, to focus on regularization algorithms, each of the turns is characterized by a different current value, controlled by a specific current supply.

2.2 Current synthesis problem

The aim of the problem is to select the n_t currents to generate a uniform flux density map with a prescribed value $\mathbf{B}_0$, uniform within the coil in a region adjacent to the symmetry

plane $z = 0$ and with an amplitude as small as possible outside the winding. In such a situation, it is reasonable to limit the search for the best current distribution to configurations symmetric with respect to the plane $z = 0$, thus reducing the unknown currents to just $n_t/2 = 10$.

To evaluate the field uniformity in the inner region of interest (ROI), the magnitude of the trial flux density field **B** is sampled over $n_p = 30$ field points, evenly spaced on the boundary of the ROI (lines S_1, S_2 and S_3 in Figure 1); on the other hand, to guarantee the minimum field amplitude in the outer region, the field is sampled on $n_k = 10$ points along the line γ in Figure 1. More details on the benchmark problem geometry can be found in Di Barba *et al.* (2020).

Starting from this background, the field synthesis problem is defined as:

> *[. . .] find the current distribution I that minimizes the discrepancy between the actual induction field* **B**(r, z) *and the prescribed field* $\mathbf{B}_0$(r, z)

where $\mathbf{B}_0 = (B_{r0}, B_{z0})$; $B_{r0} = 0$ and $B_{z0} = K$ along S_1 and S_2; $B_{z0} = K$ along S_3; $B_{z0} = 0$ along γ; K represents the desired field level (2.00 mT is assumed in the present work) and advantage is taken from symmetry being $B_{r0} = 0$ on the axis $r = 0$.

By exploiting the linearity of the relation between magnetic field and current in the forward problem, the current synthesis problem can be tackled and solved in terms of an inverse problem governed by a rectangular matrix, usually called the *lead field* matrix. The lead field matrix exhibits as many columns as unknown currents and as many rows as the number of measured flux densities. For the sake of data availability, the computed lead field matrix is reported in Appendix 1.

Accordingly, several methods for solving a rectangular system of equations are considered in a comparative way.

3. Properties of the lead field matrix

The synthesis criteria defined in Section 2.2 can be recast in terms of field component values in several "control points" along curves S_1, S_2, S_3 and γ; under these hypotheses, the computation of the magnetic field in the control points can be described using a matrix $\underline{\underline{A}}$:

$$\underline{\underline{A}} \quad \mathrm{I} = \mathrm{m} \tag{1}$$

where $\underline{I}$ is the array of unknown currents, $\underline{m}$ is the array of field data (called "measurements" in the following, to comply with the jargon of inverse source problems) and $\underline{\underline{A}}$ is the lead field matrix, linking the currents in the coils and the field values in the measurement points, can be computed either analytically (Urankar, 1982) or by using numerical methods. As mentioned before, in this paper, we compute $\underline{\underline{A}}$ using an FE approach, assuming a two-dimensional (2D) axial symmetric model and exploiting the symmetry along the z plane to reduce the computational area to only the upper part of the geometry.

In this section, we will present the most relevant characteristics of the matrix $\underline{\underline{A}}$, together with a correlation analysis of the input data (the currents in the coil) and of the output data (the flux density components in the test points), based on a database of 10,000 random samples of ten currents.

The measurements are given in ten points along S_1 (20 measurements in total, as $B_{r0} = 0$ and $B_{z0} = K$ in each point along S_1), ten points along S_2 (again, 20 measurements), ten points along S_3 (but just 10 measurements, as $B_{r0} = 0$ by definition) and finally, ten points along g (again, $B_{r0} = 0$ on γ). A picture of the target field measurements is reported in Figure 2.

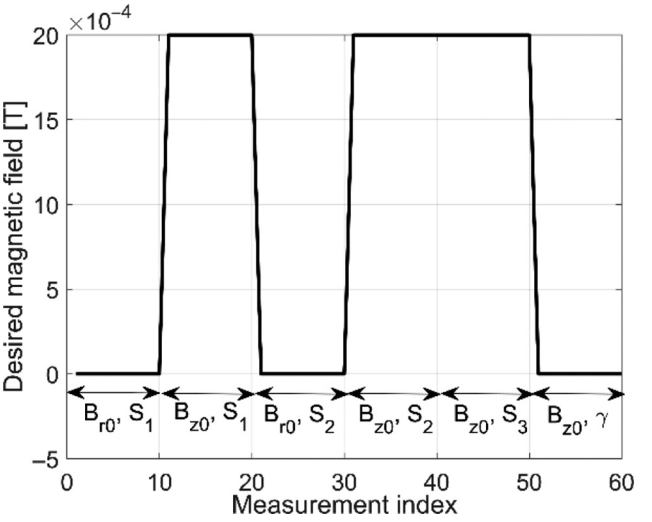

Figure 2.
Target field values on lines S1, S2, S3 and γ, put together according to a measurement index

The matrix $\underline{\underline{A}}$ has ten columns (as many as independent currents) and 60 rows (as many as considered flux density "measurements"). Its rank is ten, and its conditioning number is 7.9×10^4, which suggests an ill-conditioned problem. Moreover, the conditioning number sets a lower bound on the solution error associated with direct methods (Section 4).

The distribution of the singular values is reported in Figure 3, while the right singular vectors, which form the basis of currents algebraic space defined by the singular values decomposition, are reported in Figure 4.

It can be noted that the "natural" field distributions corresponding to low-order modes in the current base are associated to prevalently z-directed fields both inside and just outside

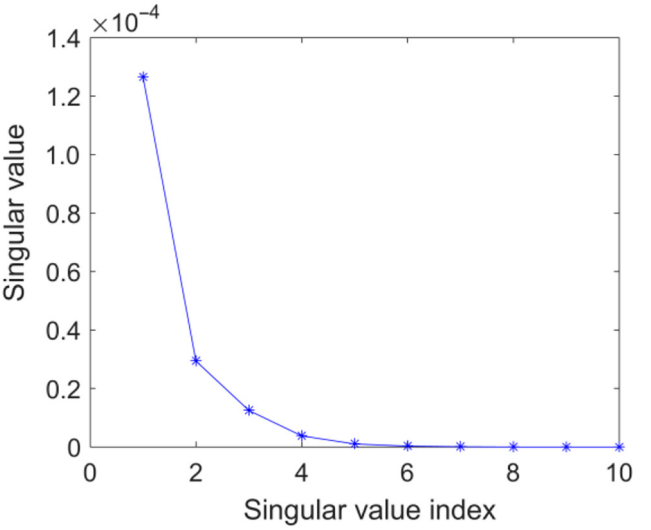

Figure 3.
Singular values of the lead field matrix $\underline{\underline{A}}$

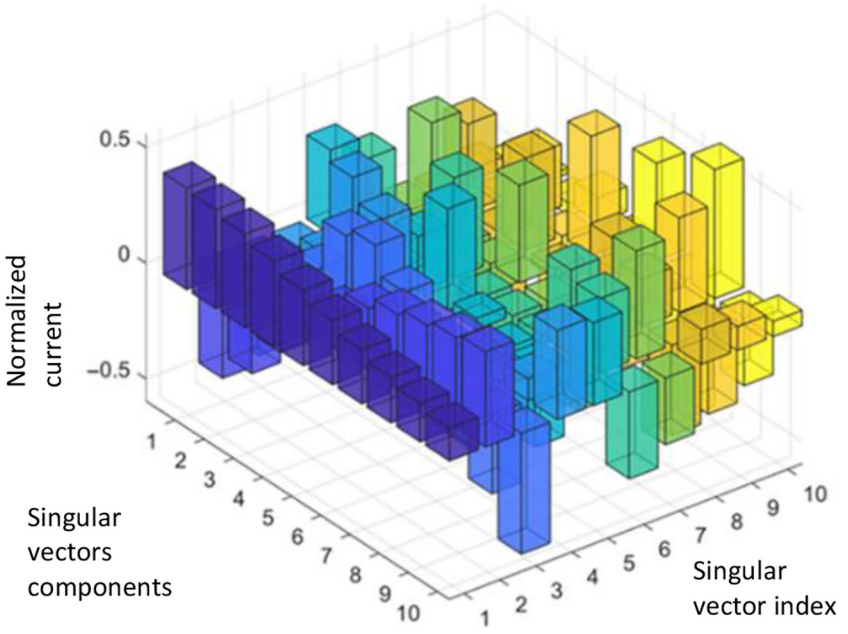

Figure 4.
Right singular vectors of $\underline{\underline{A}}$

the solenoid. By contrast, the problem definition requires a vanishing B_{z0} just at its outer edge, making the problem of finding currents quite hard to solve if not using all current modes.

The inverse problem is shown to be ill-conditioned also by looking at the principal component analysis (PCA) (Jolliffe, 2002) of the input (currents) and output (flux densities) spaces. By using 10,000 randomly generated current distributions and computing the flux densities by multiplying by $\underline{\underline{A}}$, a database of 10,000 samples of input–output couples are built and then statistically analyzed. The representation of the covariance matrix for the currents is reported in Figure 5(a) and percentage of variance of data fitted by a model with increasing number of retained principal components is reported in Figure 5(b). Note that the covariance matrix is mostly diagonal; in this case, almost all ten currents reveal to be necessary.

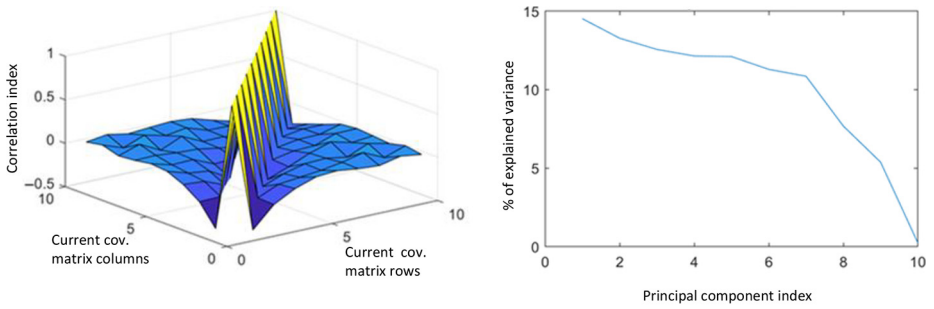

(a) (b)

Figure 5.
(a): Covariance matrix for currents in the sample database. (b): Percentage of fitted variance using reduced set of components in the PCA

The situation is rather different when analyzing the output space (the flux density values). The covariance matrix is reported in Figure 6(a), while the percentage of variance of data fitted by a model with increasing number of retained principal components is reported in Figure 6(b). The situation is now pretty different with respect to Figure 5(b). The data on the flux density measurements are correlated, because they can be derived from a single components vector potential, thanks to symmetry and Maxwell's equations; thus, the measurements are redundant, as the highly symmetric geometry makes the r and z components of the field correlated. This is also shown by Figure 6(b), showing that just five principal components of the measured flux densities array are sufficient to explain 95% of data variance.

Note that the benchmark nature of the considered problem justifies the redundant nature of the output space, because the problem characteristics allow the maximum range of action to regularizing approaches, including a model reduction approach to simplify the input–output relationship.

4. Regularization methods

The focus of this paper is on the proposal of a benchmark problem for source synthesis problems, which were introduced in Section 2. In this section, we present a comparative review of some among the best-known regularization methods and their application to the proposed current synthesis problem. We will be considering the following schemes:

- *Classical (direct) methods*: Tikhonov method, truncated SVD principle, n-method, Kaczmarz method; and
- *Statistical methods*: Linear regression, linear fit with PCA, elastic net regularization.

The classical and statistical methods considered here are based on the properties of the lead field matrix $\underline{\underline{A}}$, computed using field equations via FE analysis.

4.1 Direct methods

The regularization of linear inverse problems $\underline{I} = \underline{\underline{A}}^{-1}\underline{m}$, where $\underline{\underline{A}}^{-1}$ represent the (pseudo-) inverse of $\underline{\underline{A}}$, is a classical topic in the literature on inverse problems, and quite many different approaches have been proposed in literature. Starting from the classical Tikhonov approach [TA, (Neittaanmäki *et al.*, 1996)], the truncated singular value decomposition [SVD, (Neittaanmäki *et al.*, 1996)] and the discrepancy principle [DP, (Morozov, 1984)], until more recent "iteration-based" methods, such as the ν-method [νM, (Brakhage, 1987)] or the

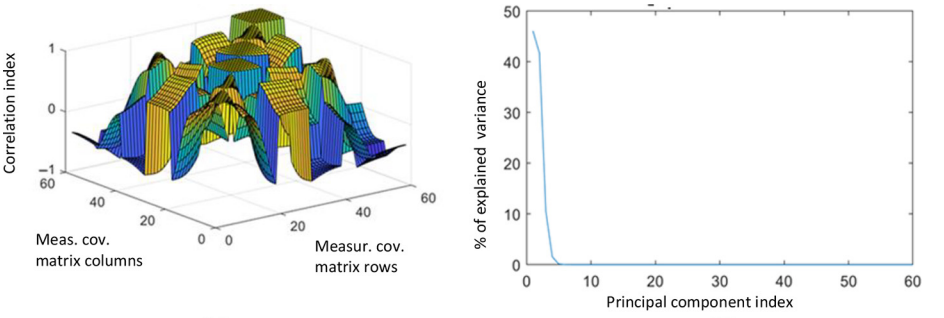

Figure 6.
(a): Covariance matrix for measurements in the sample database. (b): Percentage of fitted variance using reduced set of components in the PCA

ART method (Natterer and Wübbeling, 2001). This list is in no way exhaustive and just represents the set of classical regularization methods adopted in this paper. A broader list of possible regularization methods can be found in Engl and Groetsch (1987), Formisano and Martone (2019) and Formisano (2005). For the readers' convenience, we provide in this section a very short description of the regularization methods.

4.1.1 Truncated approach. The TA is probably the most diffused counter measure to the ill-posed nature of inverse problems. In the notation adopted here, the solution process of the (regularized) inverse problem can be cast as:

$$\min_{\underline{I}} \left(||\underline{\underline{A}}\underline{I} - \underline{m}_B||_B + \lambda \underline{I}||_I \right) \tag{2}$$

where $\|\cdot\|_B$ represents the two-norm in the output space of measurements, $\|\cdot\|_I$ represents the two-norm in the input space of currents and λ is the "regularization parameter". The choice of λ is crucial to get a smooth yet meaningful solution. λ is usually chosen either using the λ-curve approach (Hansen, 2001) or alternatively the generalized cross-validation method (Di Barba, 2010).

The actual problem of the *TA* is, hence, to identify the value of the Tikhonov parameter λ, which gives the best trade-off between model-to-data agreement (small discrepancy) and solution norm (smooth solution). Often the best suited value of λ is obtained by a parametric analysis and plotting the solution norm. The best suited λ value is obtained at the point of maximum curvature in the L-curve, usually called the "knee" of the curve.

Other possibilities have been introduced for the norm of the solution, but the two-norm is the most common one.

4.1.2 Truncated singular value decomposition. The T-SVD is based on the representation of the lead field matrix $\underline{\underline{A}}$ in terms of its left and right singular vectors:

$$\underline{\underline{A}} = \sum_{i=1}^{N} s_i \underline{u}_i \underline{v}i^T \tag{3}$$

where $\underline{u}_i$ and $\underline{v}_i$ are ortho normal vectors in the input and output spaces, respectively (to which $\underline{I}$ and $\underline{m}$ belong), while s_i are the matrix singular values, in descending order, and N is the matrix rank. If summation is truncated to $n < \mathrm{N}$, we get a rank deficient well-conditioned matrix $\underline{\underline{A}}_{\mathrm{n}}$, whose pseudo-inverse $\underline{\underline{A}}^{-1}{}_{\mathrm{n}}$ is used to compute the solution: $\underline{I}_{\mathrm{n}} = \underline{\underline{A}}^{-1}{}_{\mathrm{n}}\, \underline{m}$. The smaller n, the fewer terms in the expansion are taken and the smoother will be the solution, so a tradeoff between smoothness and solution details must be achieved when selecting the truncation index.

4.1.3 Discrepancy principle. The DP essentially swaps the role of system error and solution norm in the TA, solving the following minimization problem to determine the solution $\underline{I}$:

$$\min_{\underline{I}} \left(||\underline{I}||_I \right) \quad subject\ to\ ||\underline{\mathrm{AI}} - \underline{m}_B||_B < \varepsilon \tag{4}$$

4.1.4 ν-method. The key idea behind the ν-method is related to the characteristic of the linear problem $\underline{\underline{A}}\underline{I} = \underline{m}$ that can be solved iteratively by applying the conjugate gradient (CG) algorithm for the (unregularized) normal equation $\underline{\underline{A}}^{\mathrm{T}}\, \underline{\underline{A}}\underline{I} = \underline{\underline{A}}^{\mathrm{T}}\, \underline{m}$. It has been observed that when using CG, the "low frequency" components of the solution tend to converge faster than higher frequency ones. This "regularizing" capability is achieved by stopping the CG

iterations to an index n less than the index required to achieve full convergence. Thus, the number of stopping iterations n has the role of a regularizing parameter. The idea behind νM is to exploit this property, yet slowing down convergence of low frequency components, to reduce the dependence on the stopping criterion.

4.1.5 Algebraic reconstruction technique. The Kaczmarz method (also known as the algebraic reconstruction technique) is an iterative method based on a row-wise correction of the trial solution $\underline{I}_k$:

$$\underline{I}_k = \underline{I}_{k-1} + \frac{\underline{m}k - \underline{A}k\underline{I}k - 1}{||\underline{A}k||^2} \tag{5}$$

The regularization parameter is again the index n. The ART method does not involve matrix inversion or even matrix multiplication, but its convergence is slower than CG or other CG-based approaches.

4.2 Statistical approaches

The idea behind this type of approach to inverse problems resolution is to extract a relationship between measurements and sources from a set of "measured" data. This is the approach typically adopted in experimental physics, when adopting a "behavioral model" (e.g. a linear relationship between two sets of data) and using the available data to fit parametrically the model to the data, in the hypothesis that the fitted model will be able to describe also unseen examples. A number of tentative models are available in literature, but for the problem at hand, it is quite natural to assume a linear fit, as knowledge about the linearity of the underlying problem is available. The major problem in this case is that the ill-conditioned nature of the problem amplifies data nuisances, and a redundant number of examples helps reducing this problem. We will analyze here a few well-known interpolation approaches:

4.2.1 Multi-linear regression (MLR). A linear regression model from multiple data m_k (k = 1, 2, . . ., M) to multiple output I_l is expressed by:

$$I_l = \beta_{l0} + \sum_{k=1.M} \beta_{lk} m_k + \varepsilon_l \; l = 1,2,\ldots N \tag{6}$$

β_0 is the constant term in the model (vanishing in the present case), β_{lk} are the interpolation coefficients, ε_l is the residual error, due to, e.g. measurement noise. In the following, the uncorrelated assumption is taken for ε_l, and for currents I_l (thus using independent fit for each current). The coefficients are estimated by minimizing the mean squared difference between the predicted and true response arrays (method of *least squares*). Under assumptions on the noise terms, these coefficients also maximize the likelihood of the prediction vector.

4.2.2 Linear fit with principal component analysis (LPCA). As easily seen from the lead field matrix analysis and from the correlation analysis of the field measurement, the information about the (required) field map is highly redundant, so any regression model should probably deal with such an issue. A robust way to ease the building of "regressors" is to use a PCA to help regularizing the inverse problem resolution when using statistical analysis. As already discussed in Section 3, the principal components may be seen as a new set of variables, each one being a *linear combination* of the original variables. All the principal components are orthogonal to each other, so there is no redundant information. The principal components as a whole form an orthogonal basis for the space of the data. The

peculiar characteristic of the new basis is that the elements can be ranked in a decreasing order of variance over the data set, so a reduced number of variables can be selected to "describe" data with any selected level of variance. Linear fit of outputs is then performed over the reduced set of input descriptive variables.

4.2.3 Elastic net regularization (ENR). Elastic net regularization (ENR) is a regularization technique to minimize the regression coefficients of less relevant variables. For each "reconstructed" variable (currents, in our example), the ENR technique solves the following minimization problem to find the set of interpolation coefficients β_0, β_k, $k = 1...M$ (Zou and Hastie, 2005):

$$\{\beta_0, \underline{\beta}\} = \underset{\beta 0, \underline{\beta}}{argmin} \left(\frac{1}{2N_{Samples}} \sum_{i=1,N_{Samples}} \left(I_i - \beta_0 - \underline{m}_i^T \underline{\beta} \right)^2 + \lambda P_\alpha(\underline{\beta}) \right) \tag{7}$$

where $\alpha \in 0,1$, λ is a nonnegative real number and:

$$P_\alpha(\underline{\beta}) = \frac{(1-\alpha)}{2} ||\underline{\beta}||_2^2 + \alpha ||\underline{\beta}||_1 \tag{8}$$

Note that ENR for $\alpha = 1$ reduces to *lasso* regularization, while for $\alpha \to 0$, ENR approaches ridge regression.

5. Artificial neural network approach

As a further alternative to the classical regularization methods, an ANN is applied (Bernd, 1986; Vasilyev and Tarkhov, 2014). Accordingly, sources can be identified by a suitably trained ANN. This strategy for inverse problem-solving is rather common and requires a data set composed by the parameters and solutions for the problem (either in direct or inverse form). Training an ANN on this data set teaches the network the functional relationship between parameters and solutions, thus creating a black-box solver of the inverse problem.

In fact, an ANN-based method intends to address the solution of the synthesis problem based on an equation-free model; while classical methods here considered are based on the properties of the lead field matrix, ANN-based methods are driven by a big collection of purely numerical data, which represent the available knowledge of the direct problem.

For the purpose of this work, the inputs of the ANN are the field measurements and the outputs of the ANN are the current sources. A single k-th element of the data set is composed by a 1×10 column vector of currents I_k and a 1×60 column vector of measurements m_k. The numerical nature of the inverse problem is a linear LSQ problem, for which the ordinary solution is $I_k = \left(\underline{A}^{\mathrm{T}} \underline{A}\right)^{-1} \underline{A}^{\mathrm{T}} m_k$. Indeed, the ordinary solution is not advisable considering the ill-conditioning of the problem, but it still gives a clear insight on the linear nature of the inverse problem. Because the here discussed inverse problem is linear, a feed-forward NN architecture, with a single hidden layer and linear activation function, has been chosen. The data set used for the training of the neural network consists of 500 examples of current distributions and the corresponding magnetic field profiles. As all neurons have a linear activation function, the training procedure is a linear problem as well. For this reason, the only quantity monitored to halt the training algorithm is the performance in terms of mean absolute error (MAE).

6. Results

In this section, we present the results obtained by different regularization approaches, grouped by the regularization method class (direct, statistical, heuristics) to ease readability.

6.1 Classical regularization methods

To find the knee point of the L-shaped curve, the discrepancy function:

$$f(\lambda) = ||\underline{\underline{A}}\,\underline{I}_\lambda - \underline{m}||^2 - \frac{||\underline{I}\lambda||^2}{||\underline{I}g||^2} \tag{9}$$

subject to:

$$(\underline{\underline{A}}^T\underline{\underline{A}} + \lambda\,\underline{\underline{1}})\,\underline{I}_\lambda = \underline{\underline{A}}^T\underline{m} \tag{10}$$

and where $\underline{I}_g$ is a guessed solution (e.g. the one found by means of the SVD method), is plotted versus λ (Figure 7).

By minimizing equation (9), the knee point of the L-curve is found for λ Tik = 2.5 10^{-9}.

The magnetic field B_{Tik} reconstructed using the value of the knee point is represented in Figure 8.

Both SVD and truncated SVD approaches have been used. The truncated SVD has been subsequently applied, after discarding 1, 2, ., 8 SVs, respectively.

The reconstructed induction field obtained by means of truncated SVD with 4 and 8 SVs is shown in Figure 9.

The corresponding profile of reconstructed currents, identified by means of Tikhonov's regularization and SVD method, are shown in Figure 10.

Being the maximum current allowed in the conductors about 500 A, a few currents identified by means of SVD regularization are not feasible because they exceed this value

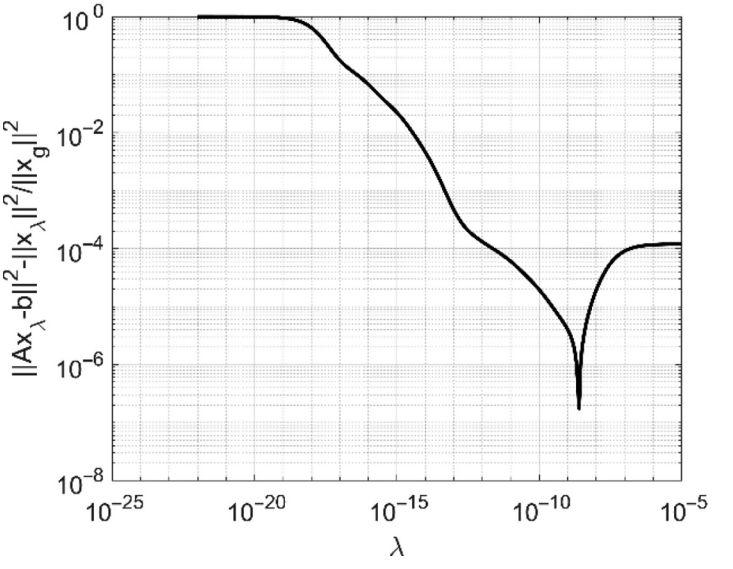

Figure 7.
Discrepancy function (3) versus λ

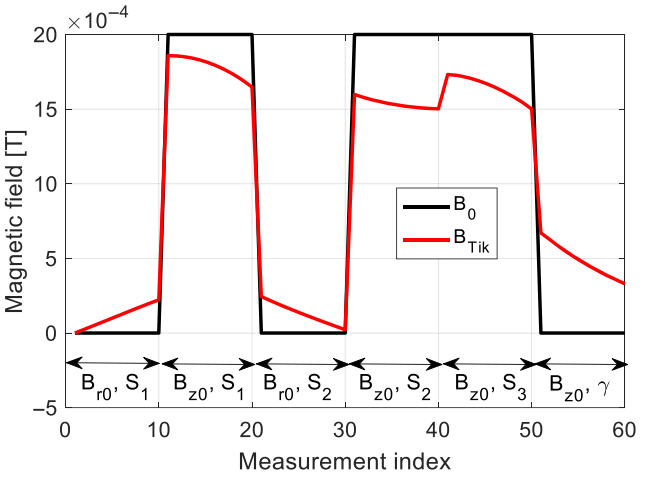

Figure 8.
Induction field reconstructed by means of Tikhonov regularization

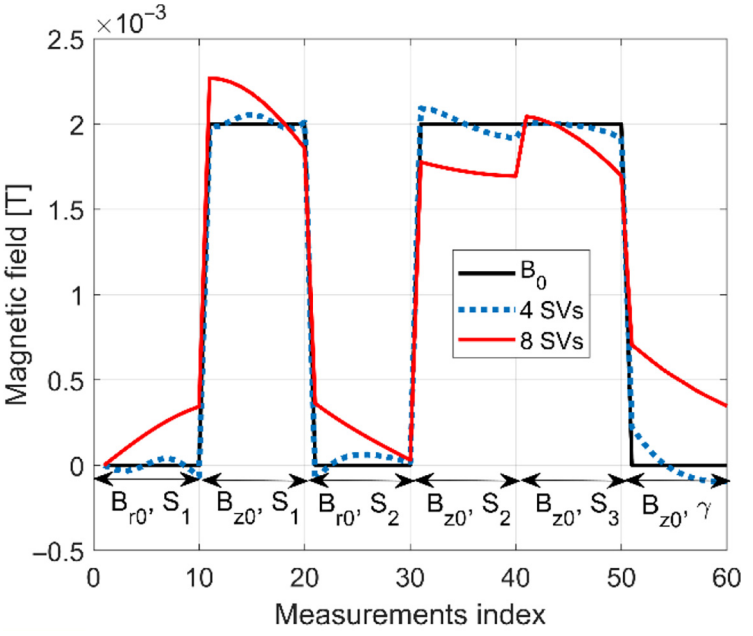

Figure 9.
Magnetic induction field reconstructed by means of truncated SVD approach

(some of them are in the order of 10^4 A). On the other hand, all the currents identified by all the other methods are feasible; at a first glance, this positive feature could be attributed to the search for a minimum energy solution achieved by Tikhonov and truncated SVD methods.

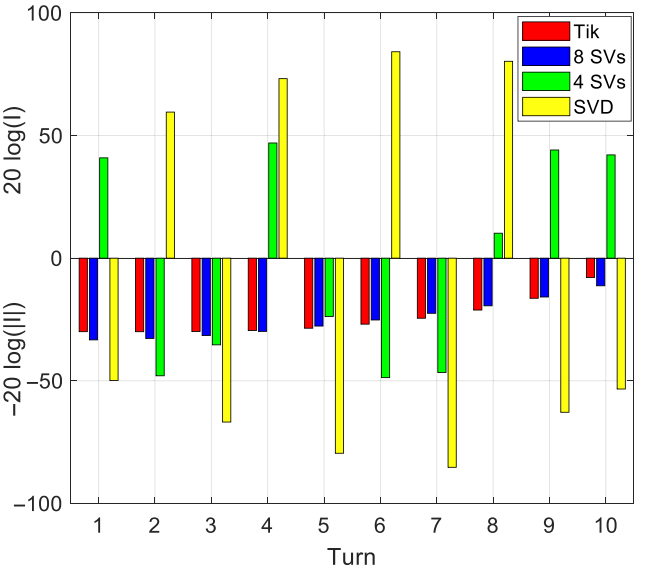

Figure 10.
Current source reconstructed by means of Tikhonov and SVD method (4SVs and 8SVs mean that 4 and 8 singular values are discarded, respectively)

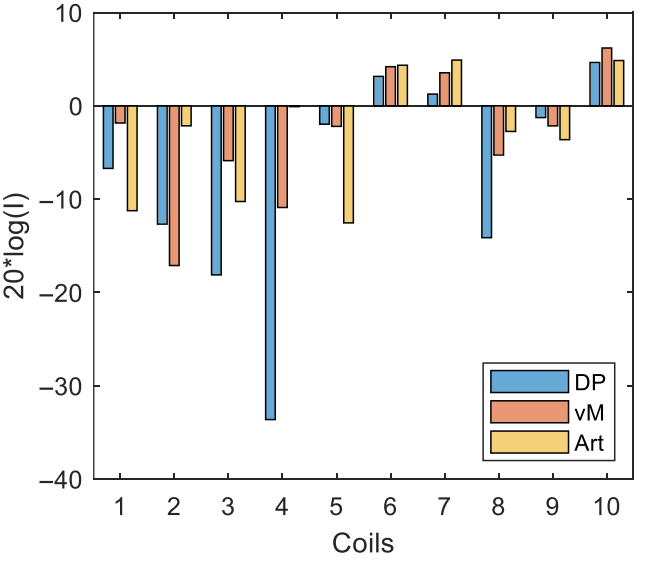

Figure 11.
Current values identified with DP, vM and ART approaches

It can be noted that, if a single copper wire is supposed to be wound and the turns are series-connected, the distribution of currents in Figure 10 represents also the distribution of the number of turns needed for each conductor.

The current values reconstructed by means of DP, νM and ART approaches are reported in Figure 11. The truncated SVD keeps five singular values.

In turn, the magnetic field profiles reconstructed along $S_k \cup \gamma$ with currents found with DP, νM and ART approaches using currents reported in Figure 11 are shown in Figure 12.

6.2 Statistical approaches

Finally, currents computed using plain multilinear regression (MLR), multilinear regression using PCA and retaining five principal components (LPCA) and finally using elastic net regularization to select most relevant measurements (ENR) are reported in Figure 13. The corresponding measurements are reported in Figure 14. Note that the highly correlated nature of the measurements allowed satisfactory results yet retaining just five principal components, while the elastic net approach, which amounts to select the most relevant measurements among the available ones, did not perform satisfactorily, as the data set used for model building did not correctly represent the actual requirements of the benchmark problem.

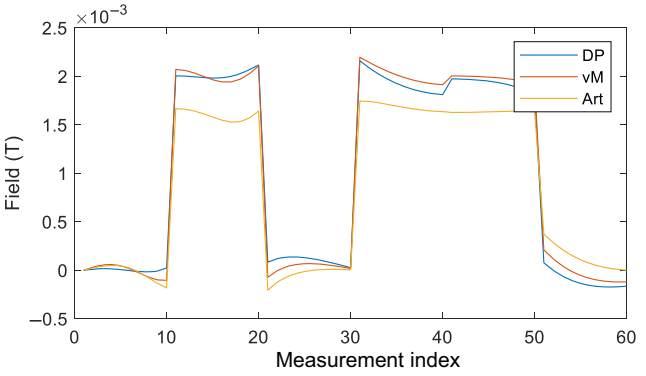

Figure 12.
Magnetic induction field profile reconstructed with DP, vM and ART approaches

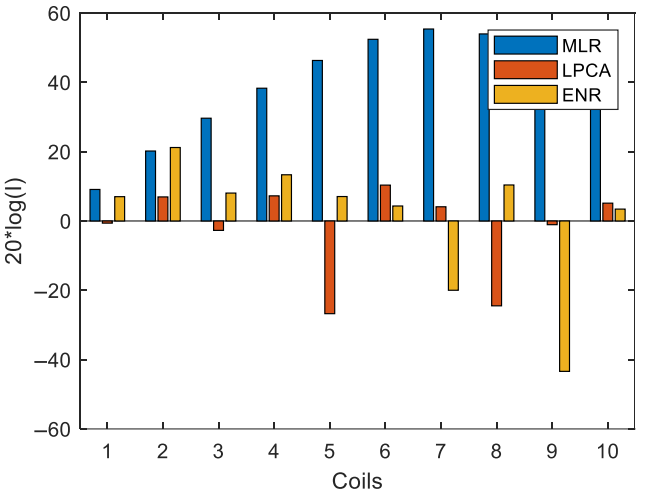

Figure 13.
Current values identified with MLR, LPCA, ENR approaches

6.3 Artificial neural network approach

For the sake of a comparison, an approach based on ANNs is here considered. Concerning the creation of the data set, a set of 500 random current vectors were created with range $\pm 10^5$A. Note that the variation range of the current is intentionally considered very broad to investigate the exploration capability of the network.

The number of samples used for this approach is definitely smaller if compared to the other methodologies presented in this work. This is because the problem presented to the neural network is purely linear and the only task that is required from the network is to learn the linear relationship between currents and fields. However, the training algorithm (the Levenberg–Marquardt, or LM) is the same regardless of the linear or non-linear nature of the problem and to work correctly, needs to express the training procedure in terms of a least-squares problem (Yu and Wilamowski, 2011). Thus, a data set of 500 samples is the minimum suitable for a LM algorithm formulation. Moreover, it is a realistic training set size that could accommodate a further expansion of the problem, including non-linearities. For each current vector, the relative measurement vector was computed through equation (2). The choice for the upper limit of the currents magnitude is to obtain a field distribution in the range of mT. Gaussian distribution was used independently for all the currents; thus, each current has 500 samples.

Thus, the complete data set is composed by 500 × 60 inputs and 500 × 10 outputs. This data set (addressed from now as the "training set") is representative for the physical system, but is essentially random and not representative for the synthesis problem. For this reason, an additional validation data set (not used for the ANN training) was created with ten waveforms obtained by scaling the one shown in Figure 2. The performance of the ANN is evaluated against the training and validation set independently. The precision of the ANN is quantified through the MAE between two reconstructed fields. The first one is reconstructed using the currents computed by the ANN. The second one is reconstructed using the currents computed by the LSQ ordinary solution. Once the error metric has been defined, the optimal sizing of the ANN is a progressive approach (Riganti Fulginei *et al.*, 2013). For the simple ANN used in this work, the only degree of freedom is the number of neurons in the hidden layer. Thus, a statistical observation of the training and validation error is performed for an increasing number of neurons. The operation is repeated and averaged with a random re-creation of the data set to compensate for bad initial conditions or non-inclusive training sets. The training results are shown in Figure 15. As can be seen, a

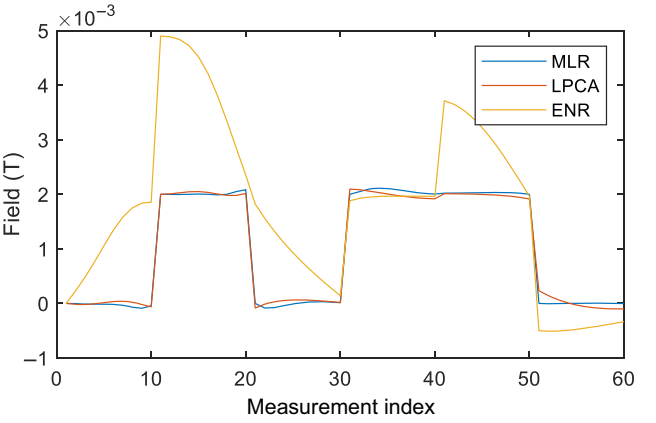

Figure 14.
Magnetic field profile reconstructed with MLR, LPCA, ENR approaches

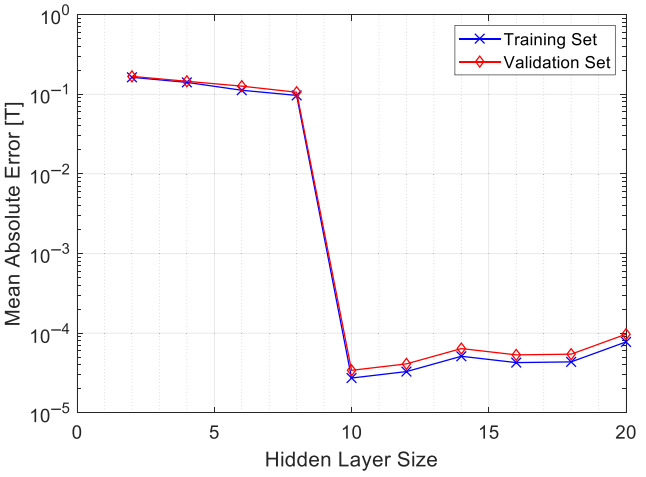

Figure 15.
MAE trend for the training (blue) and validation (red) sets for increasing number of neurons

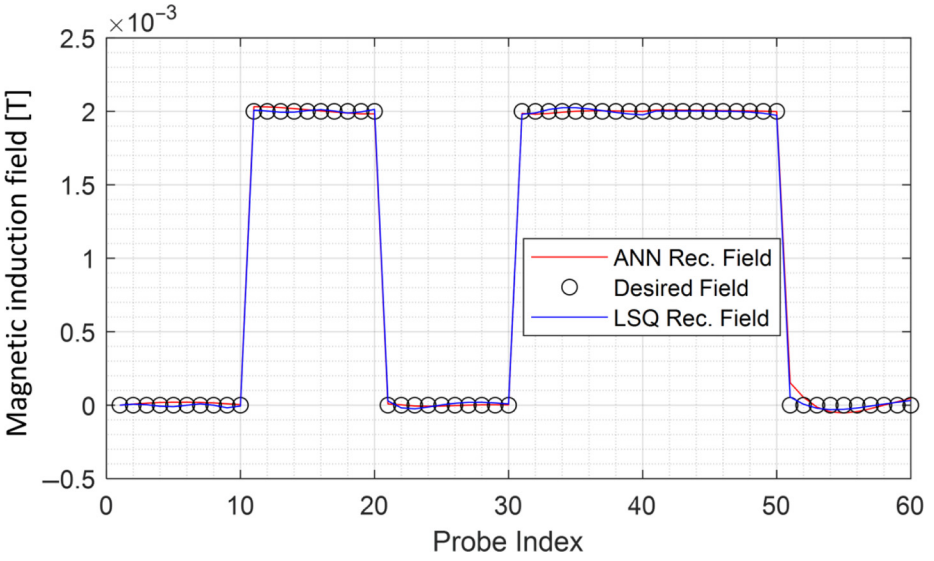

Figure 16.
Comparison between the reconstructed fields from the network and from the LSQ ordinary solution

steep change in the MAE for both training and validation set can be seen at ten neurons. The error slightly rises beyond this threshold, due to slower training convergence (Laudani *et al.*, 2015). Hence, the optimal size for the ANN hidden layer is set to 10. An example of the reconstructed field, considering B = 2.0 mT in the uniform sampling points, is shown in Figure 16. Concerning the training computational times, they are extremely reduced due to the linear activation function of the neurons. Convergence is statistically achieved in less than 100 epochs that requires, on a Core i7 machine running Matlab 2020, less than 10 s. The last aspect to take into account is the solution stability with respect to a noisy input. On this

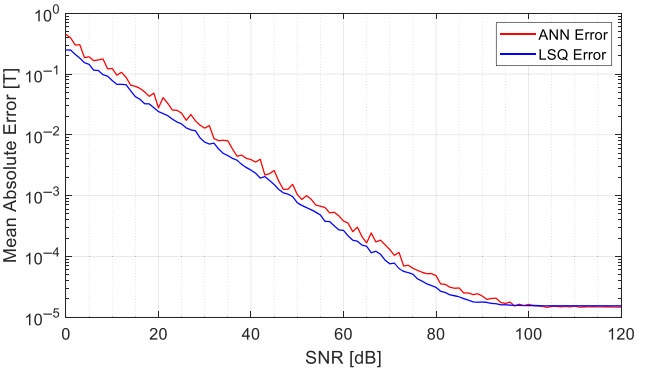

Figure 17.
MAE trend versus SNR for a noisy desired field

matter, considering a base desired field as the one in Figure 16, a white Gaussian noise was added to the non-zero sampling points. The MAE reported in Figure 17 is with respect to the non-noisy field distribution. The error for the ordinary LSQ solution is reported as well for comparison, showing that the ANN is slightly less robust than the LSQ with respect to noise.

Tables with reconstructed current values for each method are reported in Appendix 2.

7. Conclusion

Benchmark problems should find a compromise between problem solutions, that should be easy to enable many scientists to test them, but, at the same time, highlighting a peculiar difficulty in the solution, thus being an adequate test bench for different algorithms. The proposed benchmark shows that even in the case of quite simple geometries – and straightforward analysis tasks – complicated inverse problems may arise and quite different results are obtained, depending on the adopted regularization strategy. Various optimization algorithms may, therefore, be tested against the proposed benchmark. Accordingly, in the paper, a comparison of a few regularization methods is presented; while most of the "classical" methods depend on parameters able to make solution smoother at the expense of discrepancy on data, statistical-based methods depend on the choice of learning data set and its congruence with actual data for the problem at hand. Similarly, machine learning approaches provide quite effective inverse problem resolution methods, but they tend to be time consuming both in the data generation and in the training step.

Solutions of the proposed benchmark with different numerical methods and results obtained by different authors are welcome, to set up a reference collection of data in the area of inverse magnetostatics.

References

Bernd, H. (1986), *Regularization for Applied Inverse and Ill-Posed Problems: A Numerical Approach*, Springer, Berlin, ISBN 978-3-322-93034-7.

Brakhage, H. (1987), "On ill-posed problems and the method of conjugate gradients", in Engl, H.W. and Groetsch, G.W. (Eds), *Inverse and Ill-Posed Problems*, Academic Press, New York, NY.

Di Barba, P. (2010), *Multiobjective Shape Design in Electricity and Magnetism Lecture Notes in Electrical Engineering*, Springer, Berlin, ISBN 978-90-481-3080-1.

Di Barba, P., Dughiero, F., Forzan, M., Lowther, D.A., Mognaschi, M.E., Sieni, E. and Sykulski, J.K. (2020), "A benchmark TEAM problem for multi-objective pareto optimization in magnetics: the time-harmonic regime", *IEEE Transactions on Magnetics*, Vol. 56 No. 1, pp. 1-4.

Engl, H.W. and Groetsch, G.W. (1987), *Inverse and Ill-Posed Problems*, Academic Press, New York, NY.

Formisano, A. (2005), "Regularization of inverse magnetostatic problems: possibilities and pitfalls", *Compel – the International Journal for Computation and Mathematics in Electrical and Electronic Engineering*, Vol. 24 No. 3, pp. 740-752.

Formisano, A. (2019), "A comparison of different formulations for an inverse source magnetostatic problem", *Proc. of ACES 2019 Symposium*, *Miami, FL*, April 14-18.

Formisano, A. and Martone, R. (2019), "Different regularization methods for an inverse magnetostatic problem", *International Journal of Applied Electromagnetics and Mechanics*, Vol. 60 No. S1, pp. S49-S62.

Hansen, P.C. (1997), *Rank-Deficient and Discrete Ill-Posed Problems. Numerical Aspects of Linear Inversion*, SIAM, Philadelphia.

Hansen, P.C. (2001), "The L-curve and its use in the numerical treatment of inverse problems", in Johnston, P. (Ed.), *Computational Inverse Problems in Electrocardiology*, WIT Press, Southampton, pp. 119-142.

Isakov, V. (1990), *Inverse Source Problems*, American Mathematical Society, Providence.

Jolliffe, I.T. (2002), *Principal Component Analysis*, 2nd ed., Springer, Berlin.

Kaipio, J. and Sommersalo, E. (2005), *Statistical and Computational Inverse Problems*, Springer, Berlin.

Khan, A., Mohammadi, M.H., Ghorbanian, V. and Lowther, D.A. (2019), "Efficiency map prediction of motor drives using deep learning", *Proc. of COMPUMAG 2019 conference*, *Paris* (France), 2019.

Laudani, A., Lozito, G.M., Riganti Fulginei, F. and Salvini, A. (2015), "On training efficiency and computational costs of a feed forward neural network: a review", *Computational Intelligence and Neuroscience*, Vol. 2015 No. 4, pp. 1-13.

Morozov, V.A. (1984), *Methods for Solving Incorrectly Posed Problems*, Springer, New York, NY, Chapter 26.

Natterer, F. and Wübbeling, F. (2001), *Mathematical Methods in Image Reconstruction*, SIAM, Philadelphia.

Neittaanmäki, P., Rudnicki, M. and Savini, A. (1996), *Inverse Problems and Optimal Design in Electricity and Magnetism*, Oxford University Press, Oxford.

Riganti Fulginei, F., Laudani, A., Salvini, A. and Parodi, M. (2013), "Automatic and parallel optimized learning for neural networks performing MIMO applications", *Advances in Electrical and Computer Engineering*, Vol. 13 No. 1, pp. 3-13.

Urankar, L.U. (1982), "Vector potential and magnetic field of current-carrying finite arc segment in analytical form. Part III: exact computation for rectangular cross section", *IEEE Transactions on Magnetics*, Vol. 18 No. 6, pp. 1860-1867.

Vasilyev, A.N. and Tarkhov, D.A. (2014), "Mathematical models of complex systems on the basis of artificial neural networks", *Nonlinear Phenomena in Complex Systems*, Vol. 17 No. 3, pp. 327-335.

Yu, H. and Wilamowski, B.M. (2011), "Levenberg-Marquardt training", *Industrial Electronics Handbook*, Vol. 5 No. 12, pp. 1-16.

Zou, H. and Hastie, T. (2005), "Regularization and variable selection via the elastic net", *Journal of the Royal Statistical Society: Series B (Statistical Methodology)*, Vol. 67 No. 2, pp. 301-320.

Corresponding author
Maria Evelina Mognaschi can be contacted at: eve.mognaschi@unipv.it

Appendix 1

$-2.29\ 10^{-09}$	$-6.28\ 10^{-10}$	$3.96\ 10^{-10}$	$5.86\ 10^{-10}$	$4.90\ 10^{-10}$	$3.62\ 10^{-10}$	$2.62\ 10^{-10}$	$1.90\ 10^{-10}$	$1.40\ 10^{-10}$	$1.05\ 10^{-10}$
$-1.06\ 10^{-06}$	$-4.83\ 10^{-07}$	$3.76\ 10^{-09}$	$2.09\ 10^{-07}$	$2.49\ 10^{-07}$	$2.25\ 10^{-07}$	$1.85\ 10^{-07}$	$1.46\ 10^{-07}$	$1.13\ 10^{-07}$	$8.72\ 10^{-08}$
$-2.01\ 10^{-06}$	$-9.90\ 10^{-07}$	$-4.13\ 10^{-08}$	$3.92\ 10^{-07}$	$4.88\ 10^{-07}$	$4.47\ 10^{-07}$	$3.70\ 10^{-07}$	$2.93\ 10^{-07}$	$2.27\ 10^{-07}$	$1.75\ 10^{-07}$
$-2.78\ 10^{-06}$	$-1.52\ 10^{-06}$	$-1.77\ 10^{-07}$	$5.21\ 10^{-07}$	$7.06\ 10^{-07}$	$6.64\ 10^{-07}$	$5.55\ 10^{-07}$	$4.42\ 10^{-07}$	$3.44\ 10^{-07}$	$2.65\ 10^{-07}$
$-3.34\ 10^{-06}$	$-2.05\ 10^{-06}$	$-4.24\ 10^{-07}$	$5.69\ 10^{-07}$	$8.91\ 10^{-07}$	$8.72\ 10^{-07}$	$7.40\ 10^{-07}$	$5.93\ 10^{-07}$	$4.63\ 10^{-07}$	$3.58\ 10^{-07}$
$-3.67\ 10^{-06}$	$-2.52\ 10^{-06}$	$-7.90\ 10^{-07}$	$5.03\ 10^{-07}$	$1.02\ 10^{-06}$	$1.06\ 10^{-06}$	$9.24\ 10^{-07}$	$7.48\ 10^{-07}$	$5.87\ 10^{-07}$	$4.55\ 10^{-07}$
$-3.82\ 10^{-06}$	$-2.89\ 10^{-06}$	$-1.23\ 10^{-06}$	$3.12\ 10^{-07}$	$1.08\ 10^{-06}$	$1.23\ 10^{-06}$	$1.10\ 10^{-06}$	$9.05\ 10^{-07}$	$7.15\ 10^{-07}$	$5.56\ 10^{-07}$
$-3.82\ 10^{-06}$	$-3.14\ 10^{-06}$	$-1.70\ 10^{-06}$	$-1.94\ 10^{-08}$	$1.04\ 10^{-06}$	$1.35\ 10^{-06}$	$1.27\ 10^{-06}$	$1.06\ 10^{-06}$	$8.49\ 10^{-07}$	$6.62\ 10^{-07}$
$-3.71\ 10^{-06}$	$-3.25\ 10^{-06}$	$-2.12\ 10^{-06}$	$-4.63\ 10^{-07}$	$8.69\ 10^{-07}$	$1.41\ 10^{-06}$	$1.42\ 10^{-06}$	$1.22\ 10^{-06}$	$9.87\ 10^{-07}$	$7.75\ 10^{-07}$
$-3.53\ 10^{-06}$	$-3.26\ 10^{-06}$	$-2.45\ 10^{-06}$	$-9.64\ 10^{-07}$	$5.66\ 10^{-07}$	$1.39\ 10^{-06}$	$1.54\ 10^{-06}$	$1.38\ 10^{-06}$	$1.13\ 10^{-06}$	$8.94\ 10^{-07}$
$-1.55\ 10^{-05}$	$-1.33\ 10^{-05}$	$-1.04\ 10^{-05}$	$-7.97\ 10^{-06}$	$-6.13\ 10^{-06}$	$-4.77\ 10^{-06}$	$-3.77\ 10^{-06}$	$-3.01\ 10^{-06}$	$-2.43\ 10^{-06}$	$-1.98\ 10^{-06}$
$-1.53\ 10^{-05}$	$-1.32\ 10^{-05}$	$-1.04\ 10^{-05}$	$-8.02\ 10^{-06}$	$-6.17\ 10^{-06}$	$-4.80\ 10^{-06}$	$-3.79\ 10^{-06}$	$-3.02\ 10^{-06}$	$-2.44\ 10^{-06}$	$-1.99\ 10^{-06}$
$-1.48\ 10^{-05}$	$-1.31\ 10^{-05}$	$-1.05\ 10^{-05}$	$-8.16\ 10^{-06}$	$-6.28\ 10^{-06}$	$-4.89\ 10^{-06}$	$-3.85\ 10^{-06}$	$-3.07\ 10^{-06}$	$-2.47\ 10^{-06}$	$-2.01\ 10^{-06}$
$-1.39\ 10^{-05}$	$-1.28\ 10^{-05}$	$-1.07\ 10^{-05}$	$-8.39\ 10^{-06}$	$-6.48\ 10^{-06}$	$-5.03\ 10^{-06}$	$-3.95\ 10^{-06}$	$-3.14\ 10^{-06}$	$-2.52\ 10^{-06}$	$-2.05\ 10^{-06}$
$-1.29\ 10^{-05}$	$-1.23\ 10^{-05}$	$-1.08\ 10^{-05}$	$-8.69\ 10^{-06}$	$-6.75\ 10^{-06}$	$-5.23\ 10^{-06}$	$-4.09\ 10^{-06}$	$-3.24\ 10^{-06}$	$-2.60\ 10^{-06}$	$-2.10\ 10^{-06}$
$-1.18\ 10^{-05}$	$-1.17\ 10^{-05}$	$-1.08\ 10^{-05}$	$-9.02\ 10^{-06}$	$-7.09\ 10^{-06}$	$-5.49\ 10^{-06}$	$-4.28\ 10^{-06}$	$-3.38\ 10^{-06}$	$-2.70\ 10^{-06}$	$-2.18\ 10^{-06}$
$-1.07\ 10^{-05}$	$-1.10\ 10^{-05}$	$-1.07\ 10^{-05}$	$-9.33\ 10^{-06}$	$-7.48\ 10^{-06}$	$-5.81\ 10^{-06}$	$-4.52\ 10^{-06}$	$-3.55\ 10^{-06}$	$-2.82\ 10^{-06}$	$-2.27\ 10^{-06}$
$-9.68\ 10^{-06}$	$-1.01\ 10^{-05}$	$-1.04\ 10^{-05}$	$-9.57\ 10^{-06}$	$-7.92\ 10^{-06}$	$-6.20\ 10^{-06}$	$-4.81\ 10^{-06}$	$-3.76\ 10^{-06}$	$-2.97\ 10^{-06}$	$-2.38\ 10^{-06}$
$-8.71\ 10^{-06}$	$-9.25\ 10^{-06}$	$-9.87\ 10^{-06}$	$-9.66\ 10^{-06}$	$-8.34\ 10^{-06}$	$-6.64\ 10^{-06}$	$-5.15\ 10^{-06}$	$-4.01\ 10^{-06}$	$-3.15\ 10^{-06}$	$-2.51\ 10^{-06}$
$-7.83\ 10^{-06}$	$-8.40\ 10^{-06}$	$-9.23\ 10^{-06}$	$-9.56\ 10^{-06}$	$-8.72\ 10^{-06}$	$-7.13\ 10^{-06}$	$-5.56\ 10^{-06}$	$-4.31\ 10^{-06}$	$-3.37\ 10^{-06}$	$-2.67\ 10^{-06}$
$-3.31\ 10^{-06}$	$-3.17\ 10^{-06}$	$-2.65\ 10^{-06}$	$-1.46\ 10^{-06}$	$1.37\ 10^{-07}$	$1.25\ 10^{-06}$	$1.61\ 10^{-06}$	$1.52\ 10^{-06}$	$1.27\ 10^{-06}$	$1.02\ 10^{-06}$
$-2.90\ 10^{-06}$	$-2.73\ 10^{-06}$	$-2.23\ 10^{-06}$	$-1.23\ 10^{-06}$	$1.56\ 10^{-08}$	$9.44\ 10^{-07}$	$1.31\ 10^{-06}$	$1.30\ 10^{-06}$	$1.13\ 10^{-06}$	$9.19\ 10^{-07}$
$-2.52\ 10^{-06}$	$-2.34\ 10^{-06}$	$-1.87\ 10^{-06}$	$-1.04\ 10^{-06}$	$-5.35\ 10^{-08}$	$7.12\ 10^{-07}$	$1.07\ 10^{-06}$	$1.10\ 10^{-06}$	$9.84\ 10^{-07}$	$8.16\ 10^{-07}$
$-2.15\ 10^{-06}$	$-1.97\ 10^{-06}$	$-1.56\ 10^{-06}$	$-8.81\ 10^{-07}$	$-9.27\ 10^{-08}$	$5.36\ 10^{-07}$	$8.58\ 10^{-07}$	$9.23\ 10^{-07}$	$8.44\ 10^{-07}$	$7.11\ 10^{-07}$
$-1.80\ 10^{-06}$	$-1.64\ 10^{-06}$	$-1.29\ 10^{-06}$	$-7.36\ 10^{-07}$	$-1.10\ 10^{-07}$	$4.01\ 10^{-07}$	$6.83\ 10^{-07}$	$7.59\ 10^{-07}$	$7.09\ 10^{-07}$	$6.07\ 10^{-07}$
$-1.47\ 10^{-06}$	$-1.33\ 10^{-06}$	$-1.04\ 10^{-06}$	$-6.01\ 10^{-07}$	$-1.10\ 10^{-07}$	$2.97\ 10^{-07}$	$5.34\ 10^{-07}$	$6.09\ 10^{-07}$	$5.80\ 10^{-07}$	$5.03\ 10^{-07}$
$-1.16\ 10^{-06}$	$-1.04\ 10^{-06}$	$-8.12\ 10^{-07}$	$-4.74\ 10^{-07}$	$-9.90\ 10^{-08}$	$2.14\ 10^{-07}$	$4.04\ 10^{-07}$	$4.72\ 10^{-07}$	$4.57\ 10^{-07}$	$4.00\ 10^{-07}$
$-8.54\ 10^{-07}$	$-7.70\ 10^{-07}$	$-5.98\ 10^{-07}$	$-3.52\ 10^{-07}$	$-8.07\ 10^{-08}$	$1.48\ 10^{-07}$	$2.91\ 10^{-07}$	$3.45\ 10^{-07}$	$3.38\ 10^{-07}$	$2.99\ 10^{-07}$
$-5.62\ 10^{-07}$	$-5.06\ 10^{-07}$	$-3.92\ 10^{-07}$	$-2.32\ 10^{-07}$	$-5.60\ 10^{-08}$	$9.29\ 10^{-08}$	$1.87\ 10^{-07}$	$2.25\ 10^{-07}$	$2.22\ 10^{-07}$	$1.98\ 10^{-07}$
$-2.76\ 10^{-07}$	$-2.49\ 10^{-07}$	$-1.93\ 10^{-07}$	$-1.14\ 10^{-07}$	$-2.87\ 10^{-08}$	$4.42\ 10^{-08}$	$9.10\ 10^{-08}$	$1.10\ 10^{-07}$	$1.09\ 10^{-07}$	$9.76\ 10^{-08}$
$-7.05\ 10^{-06}$	$-7.59\ 10^{-06}$	$-8.51\ 10^{-06}$	$-9.25\ 10^{-06}$	$-8.96\ 10^{-06}$	$-7.62\ 10^{-06}$	$-6.01\ 10^{-06}$	$-4.66\ 10^{-06}$	$-3.62\ 10^{-06}$	$-2.85\ 10^{-06}$
$-7.25\ 10^{-06}$	$-7.68\ 10^{-06}$	$-8.37\ 10^{-06}$	$-8.85\ 10^{-06}$	$-8.54\ 10^{-06}$	$-7.43\ 10^{-06}$	$-6.04\ 10^{-06}$	$-4.77\ 10^{-06}$	$-3.76\ 10^{-06}$	$-2.97\ 10^{-06}$
$-7.40\ 10^{-06}$	$-7.74\ 10^{-06}$	$-8.25\ 10^{-06}$	$-8.54\ 10^{-06}$	$-8.22\ 10^{-06}$	$-7.27\ 10^{-06}$	$-6.03\ 10^{-06}$	$-4.85\ 10^{-06}$	$-3.86\ 10^{-06}$	$-3.08\ 10^{-06}$
$-7.51\ 10^{-06}$	$-7.77\ 10^{-06}$	$-8.14\ 10^{-06}$	$-8.30\ 10^{-06}$	$-7.97\ 10^{-06}$	$-7.13\ 10^{-06}$	$-6.02\ 10^{-06}$	$-4.91\ 10^{-06}$	$-3.95\ 10^{-06}$	$-3.16\ 10^{-06}$
$-7.59\ 10^{-06}$	$-7.79\ 10^{-06}$	$-8.05\ 10^{-06}$	$-8.12\ 10^{-06}$	$-7.78\ 10^{-06}$	$-7.01\ 10^{-06}$	$-5.99\ 10^{-06}$	$-4.95\ 10^{-06}$	$-4.02\ 10^{-06}$	$-3.24\ 10^{-06}$
$-7.64\ 10^{-06}$	$-7.79\ 10^{-06}$	$-7.97\ 10^{-06}$	$-7.98\ 10^{-06}$	$-7.63\ 10^{-06}$	$-6.92\ 10^{-06}$	$-5.97\ 10^{-06}$	$-4.98\ 10^{-06}$	$-4.07\ 10^{-06}$	$-3.29\ 10^{-06}$
$-7.68\ 10^{-06}$	$-7.79\ 10^{-06}$	$-7.91\ 10^{-06}$	$-7.87\ 10^{-06}$	$-7.52\ 10^{-06}$	$-6.84\ 10^{-06}$	$-5.95\ 10^{-06}$	$-5.00\ 10^{-06}$	$-4.11\ 10^{-06}$	$-3.34\ 10^{-06}$
$-7.70\ 10^{-06}$	$-7.79\ 10^{-06}$	$-7.87\ 10^{-06}$	$-7.79\ 10^{-06}$	$-7.44\ 10^{-06}$	$-6.78\ 10^{-06}$	$-5.93\ 10^{-06}$	$-5.01\ 10^{-06}$	$-4.14\ 10^{-06}$	$-3.38\ 10^{-06}$
$-7.72\ 10^{-06}$	$-7.79\ 10^{-06}$	$-7.84\ 10^{-06}$	$-7.74\ 10^{-06}$	$-7.38\ 10^{-06}$	$-6.75\ 10^{-06}$	$-5.92\ 10^{-06}$	$-5.02\ 10^{-06}$	$-4.16\ 10^{-06}$	$-3.40\ 10^{-06}$
$-7.72\ 10^{-06}$	$-7.78\ 10^{-06}$	$-7.82\ 10^{-06}$	$-7.71\ 10^{-06}$	$-7.35\ 10^{-06}$	$-6.72\ 10^{-06}$	$-5.91\ 10^{-06}$	$-5.03\ 10^{-06}$	$-4.17\ 10^{-06}$	$-3.41\ 10^{-06}$
$-1.16\ 10^{-05}$	$-1.09\ 10^{-05}$	$-9.81\ 10^{-06}$	$-8.43\ 10^{-06}$	$-7.03\ 10^{-06}$	$-5.75\ 10^{-06}$	$-4.66\ 10^{-06}$	$-3.75\ 10^{-06}$	$-3.03\ 10^{-06}$	$-2.45\ 10^{-06}$
$-1.15\ 10^{-05}$	$-1.08\ 10^{-05}$	$-9.76\ 10^{-06}$	$-8.43\ 10^{-06}$	$-7.06\ 10^{-06}$	$-5.79\ 10^{-06}$	$-4.70\ 10^{-06}$	$-3.79\ 10^{-06}$	$-3.06\ 10^{-06}$	$-2.47\ 10^{-06}$
$-1.12\ 10^{-05}$	$-1.06\ 10^{-05}$	$-9.65\ 10^{-06}$	$-8.42\ 10^{-06}$	$-7.11\ 10^{-06}$	$-5.87\ 10^{-06}$	$-4.78\ 10^{-06}$	$-3.87\ 10^{-06}$	$-3.12\ 10^{-06}$	$-2.53\ 10^{-06}$
$-1.09\ 10^{-05}$	$-1.04\ 10^{-05}$	$-9.53\ 10^{-06}$	$-8.40\ 10^{-06}$	$-7.17\ 10^{-06}$	$-5.96\ 10^{-06}$	$-4.88\ 10^{-06}$	$-3.96\ 10^{-06}$	$-3.20\ 10^{-06}$	$-2.59\ 10^{-06}$
$-1.04\ 10^{-05}$	$-1.00\ 10^{-05}$	$-9.33\ 10^{-06}$	$-8.36\ 10^{-06}$	$-7.24\ 10^{-06}$	$-6.09\ 10^{-06}$	$-5.02\ 10^{-06}$	$-4.09\ 10^{-06}$	$-3.32\ 10^{-06}$	$-2.68\ 10^{-06}$
$-9.93\ 10^{-06}$	$-9.66\ 10^{-06}$	$-9.12\ 10^{-06}$	$-8.30\ 10^{-06}$	$-7.30\ 10^{-06}$	$-6.22\ 10^{-06}$	$-5.17\ 10^{-06}$	$-4.24\ 10^{-06}$	$-3.44\ 10^{-06}$	$-2.79\ 10^{-06}$
$-9.41\ 10^{-06}$	$-9.24\ 10^{-06}$	$-8.85\ 10^{-06}$	$-8.21\ 10^{-06}$	$-7.35\ 10^{-06}$	$-6.35\ 10^{-06}$	$-5.34\ 10^{-06}$	$-4.40\ 10^{-06}$	$-3.59\ 10^{-06}$	$-2.91\ 10^{-06}$
$-8.87\ 10^{-06}$	$-8.78\ 10^{-06}$	$-8.54\ 10^{-06}$	$-8.08\ 10^{-06}$	$-7.37\ 10^{-06}$	$-6.49\ 10^{-06}$	$-5.53\ 10^{-06}$	$-4.60\ 10^{-06}$	$-3.76\ 10^{-06}$	$-3.06\ 10^{-06}$
$-8.32\ 10^{-06}$	$-8.31\ 10^{-06}$	$-8.21\ 10^{-06}$	$-7.92\ 10^{-06}$	$-7.38\ 10^{-06}$	$-6.61\ 10^{-06}$	$-5.71\ 10^{-06}$	$-4.79\ 10^{-06}$	$-3.95\ 10^{-06}$	$-3.22\ 10^{-06}$
$-7.73\ 10^{-06}$	$-7.79\ 10^{-06}$	$-7.82\ 10^{-06}$	$-7.70\ 10^{-06}$	$-7.34\ 10^{-06}$	$-6.71\ 10^{-06}$	$-5.91\ 10^{-06}$	$-5.03\ 10^{-06}$	$-4.18\ 10^{-06}$	$-3.42\ 10^{-06}$
$-2.21\ 10^{-06}$	$-2.32\ 10^{-06}$	$-2.53\ 10^{-06}$	$-2.87\ 10^{-06}$	$-3.33\ 10^{-06}$	$-3.89\ 10^{-06}$	$-4.54\ 10^{-06}$	$-5.19\ 10^{-06}$	$-5.73\ 10^{-06}$	$-6.03\ 10^{-06}$
$-2.04\ 10^{-06}$	$-2.14\ 10^{-06}$	$-2.34\ 10^{-06}$	$-2.65\ 10^{-06}$	$-3.07\ 10^{-06}$	$-3.61\ 10^{-06}$	$-4.24\ 10^{-06}$	$-4.91\ 10^{-06}$	$-5.51\ 10^{-06}$	$-5.92\ 10^{-06}$
$-1.87\ 10^{-06}$	$-1.96\ 10^{-06}$	$-2.14\ 10^{-06}$	$-2.43\ 10^{-06}$	$-2.82\ 10^{-06}$	$-3.32\ 10^{-06}$	$-3.93\ 10^{-06}$	$-4.60\ 10^{-06}$	$-5.25\ 10^{-06}$	$-5.76\ 10^{-06}$
$-1.72\ 10^{-06}$	$-1.80\ 10^{-06}$	$-1.97\ 10^{-06}$	$-2.22\ 10^{-06}$	$-2.58\ 10^{-06}$	$-3.05\ 10^{-06}$	$-3.63\ 10^{-06}$	$-4.29\ 10^{-06}$	$-4.96\ 10^{-06}$	$-5.55\ 10^{-06}$
$-1.60\ 10^{-06}$	$-1.67\ 10^{-06}$	$-1.82\ 10^{-06}$	$-2.05\ 10^{-06}$	$-2.38\ 10^{-06}$	$-2.82\ 10^{-06}$	$-3.36\ 10^{-06}$	$-4.00\ 10^{-06}$	$-4.68\ 10^{-06}$	$-5.32\ 10^{-06}$
$-1.48\ 10^{-06}$	$-1.55\ 10^{-06}$	$-1.69\ 10^{-06}$	$-1.90\ 10^{-06}$	$-2.20\ 10^{-06}$	$-2.60\ 10^{-06}$	$-3.11\ 10^{-06}$	$-3.72\ 10^{-06}$	$-4.40\ 10^{-06}$	$-5.08\ 10^{-06}$
$-1.36\ 10^{-06}$	$-1.42\ 10^{-06}$	$-1.54\ 10^{-06}$	$-1.74\ 10^{-06}$	$-2.01\ 10^{-06}$	$-2.38\ 10^{-06}$	$-2.85\ 10^{-06}$	$-3.42\ 10^{-06}$	$-4.08\ 10^{-06}$	$-4.77\ 10^{-06}$
$-1.26\ 10^{-06}$	$-1.32\ 10^{-06}$	$-1.43\ 10^{-06}$	$-1.60\ 10^{-06}$	$-1.85\ 10^{-06}$	$-2.19\ 10^{-06}$	$-2.62\ 10^{-06}$	$-3.16\ 10^{-06}$	$-3.79\ 10^{-06}$	$-4.48\ 10^{-06}$
$-1.17\ 10^{-06}$	$-1.22\ 10^{-06}$	$-1.32\ 10^{-06}$	$-1.48\ 10^{-06}$	$-1.71\ 10^{-06}$	$-2.02\ 10^{-06}$	$-2.42\ 10^{-06}$	$-2.92\ 10^{-06}$	$-3.52\ 10^{-06}$	$-4.20\ 10^{-06}$
$-1.08\ 10^{-06}$	$-1.13\ 10^{-06}$	$-1.22\ 10^{-06}$	$-1.36\ 10^{-06}$	$-1.57\ 10^{-06}$	$-1.85\ 10^{-06}$	$-2.21\ 10^{-06}$	$-2.67\ 10^{-06}$	$-3.24\ 10^{-06}$	$-3.89\ 10^{-06}$

Table A1.
Computed lead-field matrix (60, 10)

Appendix 2. Tables with reconstructed current values for each method

The currents in Tables A1–A3 are in ampère. Three significant digits are considered.

Turn	Tik	8SVs	4SVs	SVD
1	–31.5	–46.3	111	–311
2	–31.6	–43.3	–250	951
3	–31.3	–37.8	–58.5	$-2.19\ 10^3$
4	–29.9	–31.1	223	$4.57\ 10^3$
5	–26.8	–24.2	–15.5	$-9.50\ 10^3$
6	–22.1	–18.2	–273	$1.62\ 10^4$
7	–16.8	–13.3	–214	$-1.84\ 10^4$
8	–11.4	–9.36	3.23	$1.03\ 10^4$
9	–6.57	–6.19	161	$-1.39\ 10^3$
10	–2.48	–3.66	127	–465

Table A1. results obtained by means of Tikhonov's regularization and SVD method. 8SVs and 4SVs mean that SVD method has been applied after discarding 8 and 4 singular values, respectively

Turn	DP	νM	ART
1	–46.2	–80.9	–27.4
2	–23.2	–13.9	–78.1
3	12.4	50.8	30.7
4	2.08	28.5	99.0
5	–79.7	–77.6	–23.6
6	–144	–162	–165
7	–116	–150	–176
8	–19.7	–54.5	–72.9
9	86.5	78.1	65.9
10	171	204	175

Table A2. results obtained by means of DP, νM and ART methods

Turn	MLR	LPCA	ENR	ANN
1	–547	120	176	–29.6
2	$1.93\ 10^3$	–290	–214	–52.2
3	$-4.96\ 10^3$	–2.81	132	94.3
4	$1.17\ 10^4$	194	497	–548
5	$-2.62\ 10^4$	–13.4	–177	$2.15\ 10^3$
6	$4.91\ 10^4$	–268	27.0	$-7.43\ 10^3$
7	$-6.59\ 10^4$	–210	–3.28	$1.72\ 10^4$
8	$5.45\ 10^4$	10.4	–194	$-2.40\ 10^4$
9	$-2.43\ 10^4$	99.8	2.89	$1.68\ 10^4$
10	$4.59\ 10^3$	177	214	$-4.49\ 10^3$

Table A3. results obtained by means of MLR, LPCA, ENR and ANN methods